## Supplementary material

# Molecular analysis of SMARD1 patient-derived cells demonstrates that nonsense-mediated mRNA decay is impaired

Michela Taiana[1]*, Alessandra Govoni[2]*, Sabrina Salani[2], Nicole Kleinschmidt[3], Noemi Galli[1], Matteo Saladini[1], Stefano Bruno Ghezzi[2], Margherita Bersani[1], Valentina Melzi[2], Roberto Del Bo[1], Oliver Mühlemann[3], Enrico Bertini[4], Valeria A Sansone[5,6], Emilio Albamonte[5], Sonia Messina[7,8], Francesco Mari[9], Elisabetta Cesaroni[10], Liliana Porfiri[10], Danilo Tiziano[11], Gian Luca Vita[8], Maria Sframeli[8], Carmen Bonanno[7], Nereo Bresolin[1,2], Giacomo P. Comi[1,2,12], Stefania Corti[1,2]°, and Monica Nizzardo[2]°**

1 Dino Ferrari Centre, Neuroscience Section, Department of Pathophysiology and Transplantation (DEPT), University of Milan

2 Foundation IRCCS Ca' Granda Ospedale Maggiore Policlinico, Neurology Unit, Milan, Italy.

3 Department of Chemistry and Biochemistry, University of Bern, CH-3012 Bern, Switzerland

4 Department of Neuroscience - Unit of Neuromuscolar and Neurodegenerative Diseases, IRCCS Bambino Gesù Children's Hospital, Rome, Italy.

5 NEuroMuscular Omnicentre (NEMO), ASST Grande Ospedale Metropolitano Niguarda, Fondazione Serena Onlus, Piazza Ospedale Maggiore, 3, 20162, Milan, Italy.

6 Department Biomedical Sciences for Health, Università degli Studi di Milano, Milan, Italy

7 Department of Clinical and Experimental Medicine, University of Messina, Messina, Italy

8 NEMO SUD Clinical Centre for Neuromuscular Disorders, Messina, Italy

9 Child Neurology Unit, Pediatric Hospital “A. Meyer”, Viale Pieraccini 24, Florence, Italy

10 Department of Child Neuropsychiatry,G. Salesi Children's Hospital-University of Ancona, Ancona, Italy.

11 Institute of Genomic Medicine, Università Cattolica del Sacro Cuore Fondazione, Policlinico Universitario Agostino Gemelli IRCCS, Rome, Italy

12 Foundation IRCCS Ca’ Granda Ospedale Maggiore Policlinico, Neuromuscular and rare diseases unit, Milan, Italy.

**Corresponding author: Neuroscience Section, Department of Pathophysiology and Transplantation (DEPT), University of Milan, Neurology Unit, IRCCS Foundation Ca’ Granda Ospedale Maggiore Policlinico, Via Francesco Sforza 35, 20122 Milan Italy. Tel: +39 0255033833; Fax: +39 0255033800; Email: monica.nizzardo1@gmail.com, ORCID ID: 0000-0001-5447-0882

**Supplementary Figure 1**

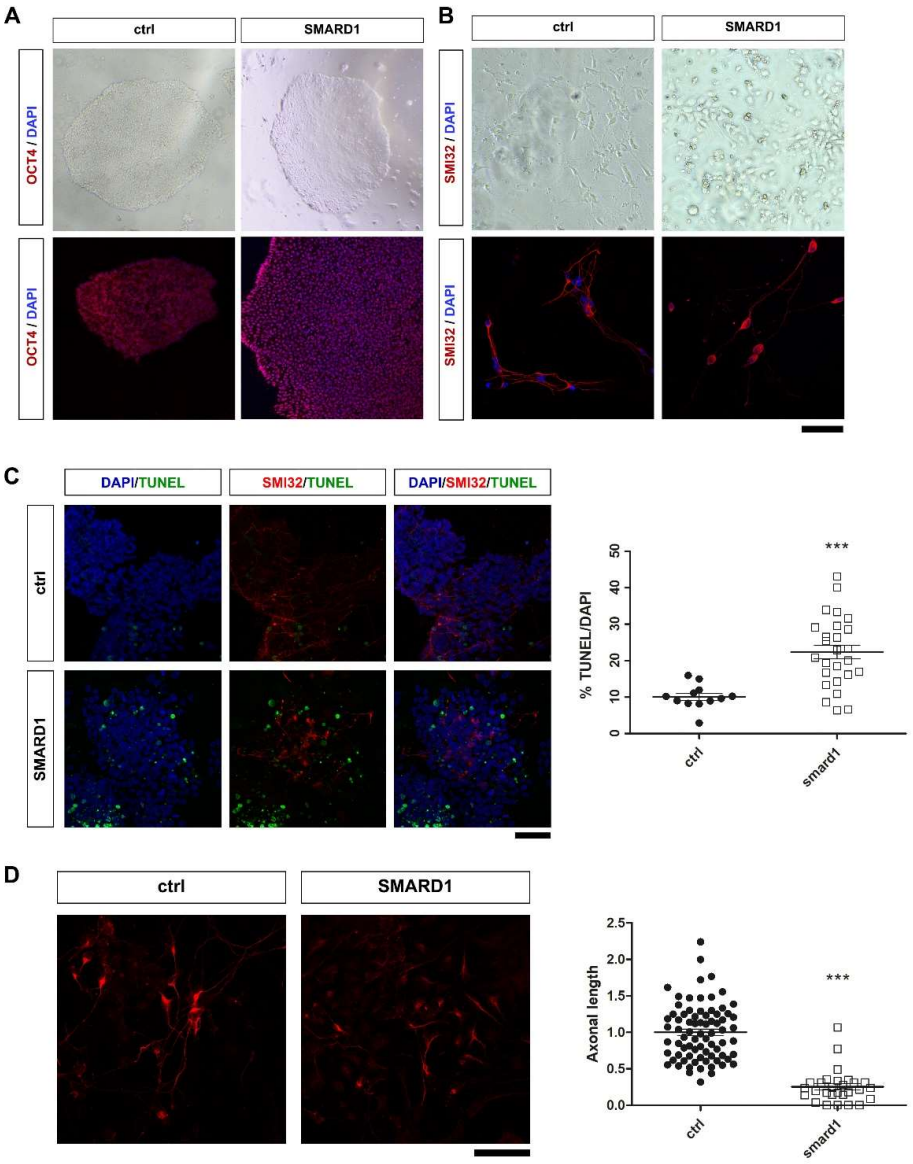


**iPSCs and MNs generation**

(A, B) Representative image of (A) the three controls (ctrl) and the four SMARD1 iPSCs colonies (brightfield upper panel) expressing specific pluripotent marker (lower panel, OCT4, red) and (B) MNs positive for MN marker (SMI32) from control (n = 3) and SMARD1 (n = 3) cases. Nuclei are

labelled with DAPI (blue). (C, D) Representative images of controls (ctrl) and SMARD1 MNs. DNA fragmentation Tunel assay showed an increased apoptosis (Tunel green, SMI32 red, DAPI, blue, **p* < 0.01, Student's t-test, n = 3 biological replicates) in SMARD1 cases. Each data point represents 1 technical replicate. (C). Quantification of MN axon length revealed a decrease in smard1 in respect with ctrl (****p* < 0.001, Student's t-test). Each point represents data from a single cell. Values are presented as means ± SEM. Scale bar: 100µm for (A, C) and 50 µm for (B, C).

**Supplementary Figure 2**

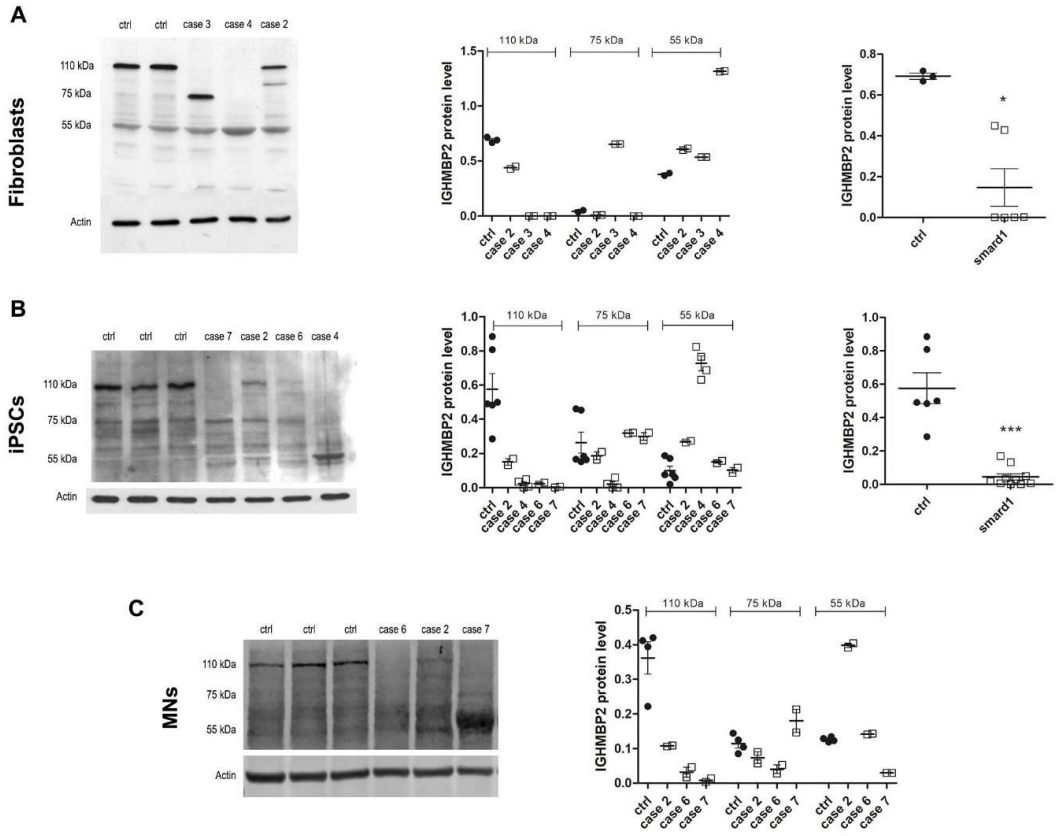


**Full-length IGHMBP2 protein is decreased in SMARD1 patient cell lines**

IGHMBP2 protein level was assessed by western blot in fibroblasts (A), iPSCs (B) and MNs (C) from patients and controls. Three different IGHMBP2 isoforms were detected at 110 kDa (full length), 75 kDa, and 55 kDa. The 110-kDa form was decreased in all SMARD1 samples, and expression of truncated forms (75 kDa and 55 kDa) varied by case. First column: representative image of western blot; second column: quantification of the protein level for each case, each data point represents 1 technical replicate; third column: quantification of the 110-kDa protein pooled for controls (ctrl) and patients (smard1). *$p < 0.05$ for fibroblasts, and ***$p < 0.001$ for iPSCs, Student's t-test. Values are presented ± SEM.

**Supplementary Figure 3**

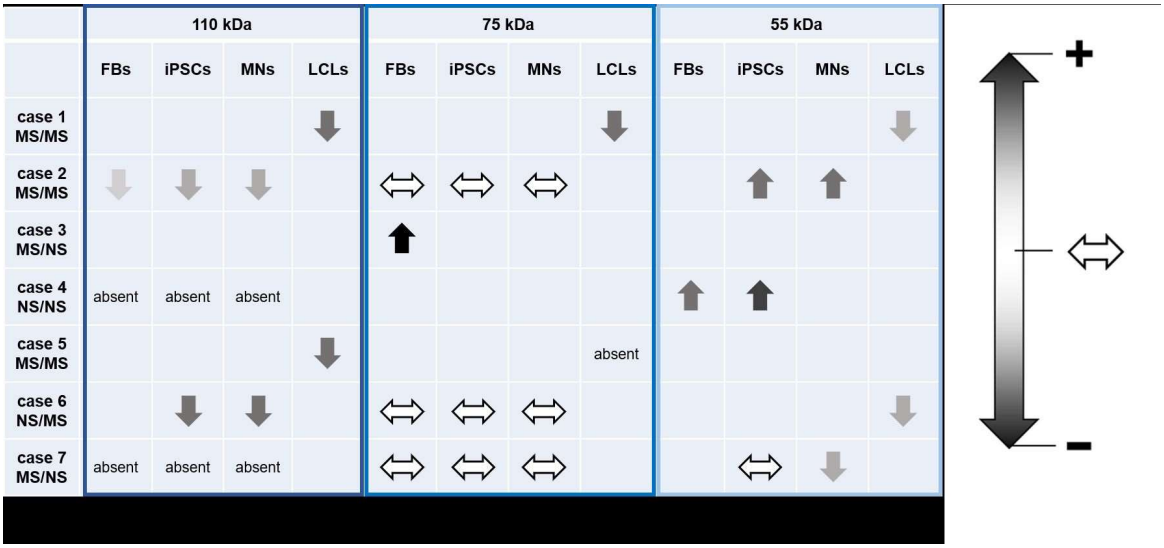


**Schematic representation of the different IGHMBP2 protein expression levels**

Schematic representation of the different IGHMBP2 protein expression levels relative to control in SMARD1 fibroblasts (FBs), iPSCs, and MNs assessed by western blot (110-kDa, 75-kDa, and 55-kDa bands). Horizontal arrows indicate unvaried protein levels, up arrows indicated increased levels, and down arrows indicate decreased levels compared to control. Greyscale shows the percentage of variation compared to control, from unvaried (white) to highest variation (black). Absent indicates undetectable protein. MS: missense, NS: nonsense.

**Supplementary Figure 4**

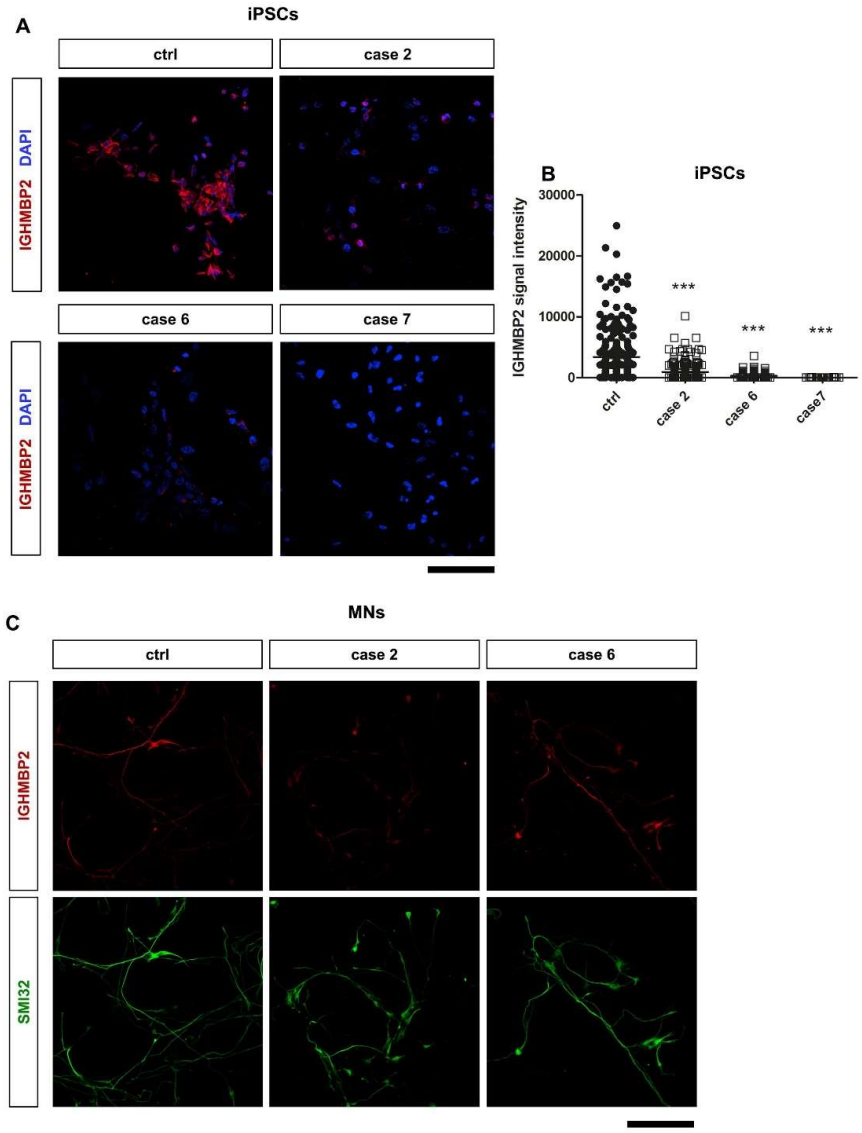


**IGHMBP2 protein is decreased in SMARD1 iPSC-derived lines**

Representative images of immunocytochemistry of iPSCs (A, DAPI in blue) and iPSC-derived MNs (C, SMI32 in green) obtained from patients with SMARD1. iPSCs showed a decrease in IGHMBP2 protein expression (red) compared to controls (ctrl). Graphs represent the immunoreactivity score quantified using ImageJ software of IGHMBP2 in iPSCs (B), n=3 technical replicates; 4 fields imaged and analyzed per replicate. Each data point represents a single cell, ***$p < 0.001$, Student's t-test, ctrl vs single case. Values are presented ± SEM.s. Scale bar: 75 µm for iPSCs and 50 µm for MNs.

**Supplementary Figure 5**

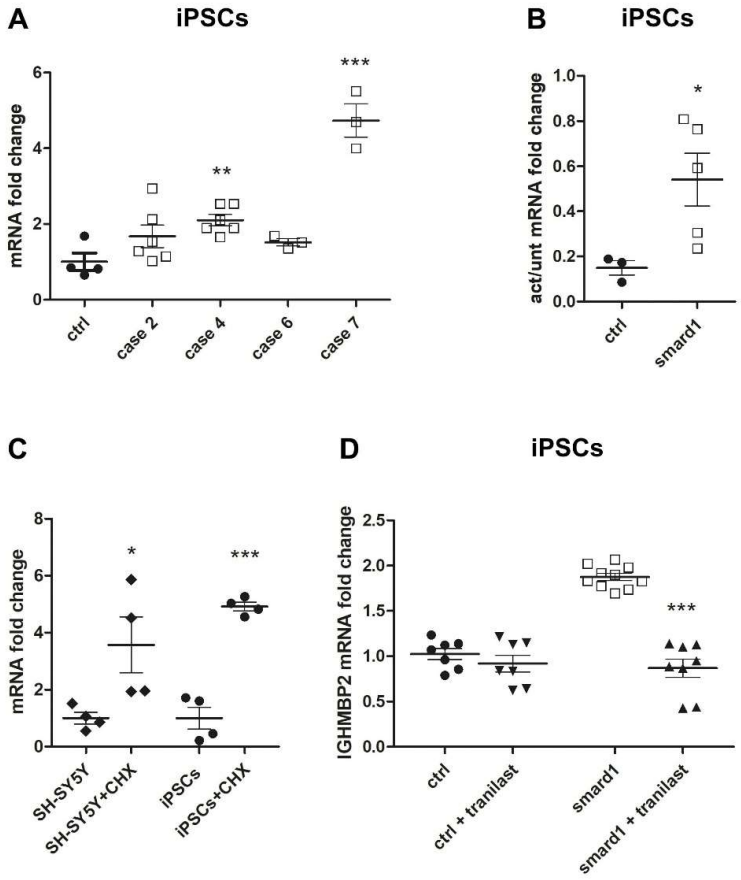


***IGHMBP2* degradation is impaired in SMARD1-derived cell lines and regulated by NMD**

qPCR analyses of *IGHMBP2* mRNA levels in iPSCs (A) showed no correlation with protein level reduction in SMARD1 cell lines and were increased compared to control (ctrl, n = 3) in specific SMARD1 cases, each data point represents a single technical replicate (**p < 0.01, ***p < 0.001, Student's t-test, ctrl vs single case). (B) Evaluation of *IGHMBP2* mRNA half-life after actinomycin D 2.5 µg/ml (act)-induced transcription inhibition revealed increased mRNA stabilization in SMARD1 iPSCs (cases 2, 6, and 7) compared to controls (n = 3), suggesting impairment of *IGHMBP2* mRNA decay, each data point represents the mean of 3 technical replicates (***p < 0.001, Student's t-test). (C) qPCR evaluation of *IGHMBP2* expression after NMD inhibition by 100 µg/ml CHX for 6 h showed a significant increase in mRNA levels compared to basal expression of untreated

cells in the neuronal cell line SHSY-5Y and in control iPSCs, suggesting NMD-mediated degradation of *IGHMBP2* mRNA, each data point represents 1 technical replicate. (*p < 0.05, ***p < 0.001, Student's t-test). (D) *IGHMBP2* mRNA level decreased in SMARD1 iPSCs after the treatment with tranilast (5 μM), an activator of NMD. n=3 biological replicates, each data point represents a single technical replicate (***p < 0.001, Student's t-test), further supporting the hypothesis that *IGHMBP2* mRNA is a target for NMD. Values are presented ± SEM.

**Supplementary Figure 6**

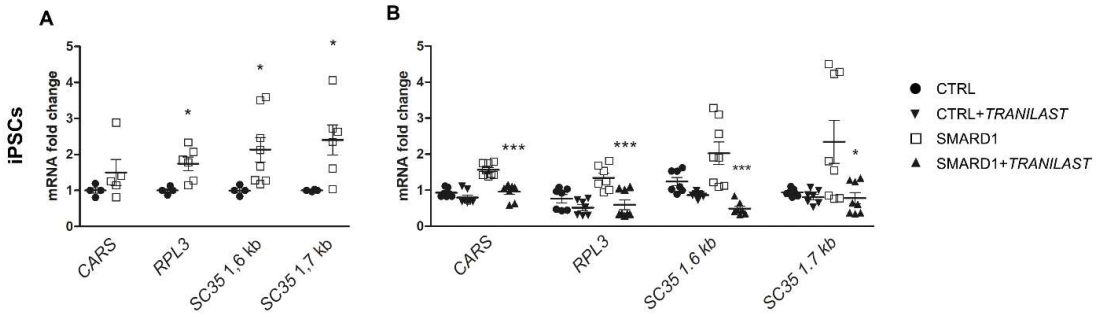


**NMD is impaired in SMARD1-derived cell lines**

(A) mRNA levels of NMD target genes were increased in SMARD1 iPSCs (cases 2, 6, and 7) compared to controls (*$p < 0.05$, Student's t-test); (B) mRNA levels of NMD target genes were rescued after treatment with tranilast (5 μM) in SMARD1 iPSCs (cases 2, 6, and 7, *$p < 0.05$, ***$p < 0.001$, Student's t-test, each data point represents a single technical replicate); Values are presented ± SEM at least from three independent experiments.

**Supplementary Figure 7**

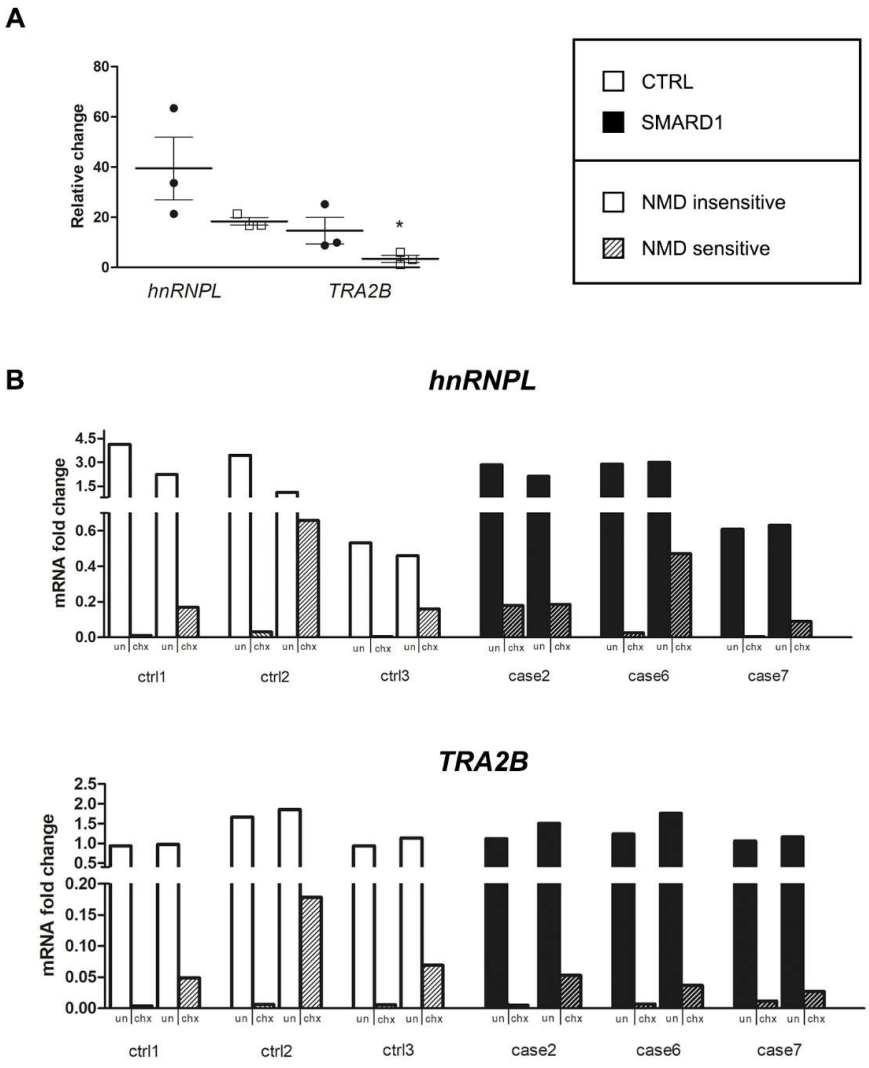


**NMD efficacy impaired in SMARD1 patients' iPSCs**

(A)Assessment of a relative increase in the NMD-sensitive isoform normalized to the NMD-insensitive isoform level of *hnRNPL* and *TRA2B* after NMD inhibition showed a reduction in NMD activity in SMARD1 iPSCs (cases 2, 6, and 7) compared to control. The ratio between $2^{-\Delta CT}$ NMD-sens/ $2^{-\Delta CT}$ NMD-ins isoforms was calculated for each sample, and its relative change after CHX treatment ((CHX-unt)/unt) was evaluated for each cell line. Each data point represents the mean of 3

technical replicate (*$p < 0.05$, Student's t-test). (B) mRNA fold change of (A) separate for each cell lines (cases 2, 6, and 7). Notably, different cases and controls presented high mRNA levels variability.

## Supplementary Table 1

| Patient (gender) | Age at onset | Motor milestone achieved | Ventilation | G-tube | Current motor ability | Mutations | Position | Reference |
|---|---|---|---|---|---|---|---|---|
| Case 1 (M) | ≤ 3 months | sitting position | tracheostomy | not now, only temporarily | tetra-paresis, minimal movements of proximal upper limbs | c.1061G>A (p.G354S) | ex 7 | [21] |
| | | | | | | c.129delC (fs) | ex 2 | |
| Case 2 (M) | ≤ 3 months | none | tracheostomy | yes | tetra-paresis, minimal movements of proximal upper limbs | c.1915G>A (p.A639T) homozygous | ex 13 | novel |
| Case 3 (F) | ≤ 3 months | poor neck control | tracheostomy | yes | tetra-paresis, antigravity movements minimally preserved at upper limbs | c.121delC (p.Q41R fsX48) | ex 2 | novel |
| | | | | | | c.439C>T (p.R147X) | ex 3 | NM_002180.2 (IGHMBP2): c.439C>T (p.R147T) |
| Case 4 (F) | > 3 months | none | tracheostomy | yes | / | c.2125C>T (p.E709X) homozygous | ex 13 | novel |
| Case 5 (F) | ≤ 3 months | none | / | no | / | 653delC (p.T218MfsX14) | ex 5 | novel |
| | | | | | | 1082T>C (p.L361P) | ex 13 | NM_002180.2 (IGHMBP2): c.1082T>C (p.L361P) |
| Case 6 (F) | > 3 months | Crawling at six months, standing position at 1 year | continuous NIV, cough assistance | yes | tetra-paresis, minimal movements of proximal upper limbs, social interactions and language skills appropriate for the age, evident tendon retraction at wrists, hip joints and ankles | c.138T>A (p.C46X) | ex 2 | [11] |
| | | | | | | c.1915G>A (p.A639T) | ex 13 | novel |
| Case 7 (M) | ≤ 3 months | none | tracheostomy | yes | tetra-paresis, minimal movements of proximal upper limbs, can communicate only by his facial mimics and eye movements | c. 86+1G>T | int 1 | novel |
| | | | | | | c. 289C>T (p.Q100X) | ex 3 | novel |
| Case 8 (F) | > 3 months | independent sitting by 14 months and ability to walk with support by 27 months | continuous NIV | yes | tetra-paresis, minimal movements of proximal upper limbs, severe rotoscoliosis | IVS 13+1G>T homozygous | / | [21] |

Clinical and genetic characteristics of the patients' cohort. Right column: mutation references.

**Supplementary Table 2**

**Characteristics of healthy donors (controls)**

| | gender | age at the sample collection |
|---|---|---|
| ctrl 1 | male | at birth |
| ctrl 2 | male | 7 years |
| ctrl 3 | male | 19 years |

## Supplementary methods

### Genetic sequencing

Blood samples from the patients were processed for the extraction of DNA. The 15 coding exons and flanking intronic regions of the *IGHMBP2* gene (NM_002180.2) were amplified by PCR, using the TaqMan Universal PCR Master Mix solution (Applied Biosystems). The amplification was performed using forward and reverse primers (Invitrogen) for each exon, as described in a previous study [1]. All PCR products were sequenced using the BigDye Terminator 3.1 protocol on an ABI-Prism 3130 Genetic Analyzer (Applied Biosystems). We conducted the sequence alignment and analysis with SeqScape software (Applied Biosystem).

### iPSC generation and differentiation

From the blood and skin biopsy specimens of patients and controls, we obtained lymphoblastoid (cases 1 and 5) and fibroblast (cases 2, 3, 4, 6, 7, 8) cells and cultured them as previously described.[41] The fibroblasts of cases 2, 4, 6 and 7 were then reprogrammed with a non-integrating viral protocol using the CytoTune®-iPS 2.0 Sendai Reprogramming Kit (Life Technologies). Spinal MNs were then obtained from wild-type and SMARD1 iPSCs following a rapid (14-days) multistage protocol that has been previously described [2].

### Western blot analyses

The cells were sonicated and centrifuged at 13,500 rpm for 10 min at 4°C. A total of 20 µg of each sample was separated using 12% SDS-PAGE and then transferred to a nitrocellulose membrane, saturated with 1% bovine serum albumin, 10% horse serum, and 0.075% Tween 20 in TBS (20 mM Tris-HCl, 0.5 M NaCl) solution for 1 h. The membrane was then incubated overnight at 4°C with the primary antibody (anti-human IGHMBP2 (1:800, Millipore) or anti-α-actin (1:250, Sigma) as loading control) in saturating solution. After 24 h, the membrane was incubated with a secondary horseradish peroxidase–conjugated antibody (Molecular Probes/Invitrogen) in saturating solution. The western

blot bands were detected via enhanced chemiluminescence (Amersham). Densitometric analysis was performed using Image J software.

**Immunocytochemistry**

Cells were fixed on coverslips in 4% paraformaldehyde, permeabilized in 0.25% Triton X-100, and blocked in 10% bovine serum albumin and 0.3% Triton X-100 in 1x PBS solution for 1 h at room temperature. After an incubation overnight with antibodies (anti-human IGHMBP2, Millipore, 1:500 dilution; SMI-32, Millipore, 1:100 dilution), cells were incubated with a 1:2000 anti-mouse immunoglobulin G Alexa Fluor 488-A11008 secondary antibody (Invitrogen) for 1 h. Detection of apoptotic cells was carried out using the terminal deoxynucleotidyl transferase dUTP nick end labelling (TUNEL) system protocol (Promega). For quantification four random fields for each sample were acquired and TUNEL positive cells were counted on the total of DAPI positive nuclei. Axonal length, detected as SMI-32–positive prolongation, was assessed considering only the longest projection completely included in the acquired field for each MN. Quantification has been performed selecting 10 random fields for each sample as previously described [3]. Quantification analysis was performed using Image J software.

## Transcript analysis

RNA extraction was performed on iPSCs and MNs derived from patients and controls, using the ReliaPrep™ RNA Cell Miniprep System kit (Promega) following the manufacturer's instructions, and dosed with NanoDrop One (ThermoFisher Scientific). Reverse-transcribed material (20 ng for each well) was amplified in triplicate using the TaqMan Universal PCR Master Mix (Applied Biosystems) and appropriate probe to evaluate *IGHMBP2* gene expression (Hs01045548_m1) by means of the ΔΔCt method on a 7500 Real Time PCR System (Software 2.01, Applied Biosystems). Expression levels were normalized to the average level of the housekeeping gene 18S (Hs99999901_s1) and referred to the relevant control samples.

With the same conditions, a qPCR analysis to quantify RNA was then performed for other transcripts known to be regulated by NMD [4], using the SYBR Green Real Time PCR Master Mix. The forward and reverse primers used were as follows: *IGHMBP2* NM-002180.2, FW 5'-GAAGACCCTGGTGGAGTATTT-3' and RW 5'-CTGGAAGTTCTCATGGGAATAG-3'); *IGHMBP2* XM-005273976.1, FW 5'-CTGCTGAAGGCCAGAAAG-3' and RW 5'-CCAGGGATGTGTCTACAGATTG-3'); *RPL3*, FW 5'-GGCATTGTGGGCTACGTG-3' and RW 5'-CTTCAGGAGCAGAGCAGA-3'); *CARS*, FW 5'-AAATTAAATGAGACCACGGA-3' and RW 5'-TGACATCACAGCCAAGTGTA-3'); *SC35 1.6kb*, FW 5'-CGGTGTCCTCTTAAGAAAATGATGTA-3' and RW 5'-CTGCTACACAACTGCGCCTTTT-3'; and *SC35 1.7kb*, FW 5'-GGCGTGTATTGGAGCAGATGTA-3' and RW 5'-CTGCTACACAACTGCGCCTTTT-3'. We also determined the relative RNA levels of the endogenous NMD-sensitive transcripts *HNRNPL_NMD* and *TRA2B_NMD* and their corresponding NMD-insensitive splice forms *HNRNPL_PROT* and *TRA2B_PROT*. For this purpose, 16 ng of the reverse-transcribed total RNA was amplified in triplicate using Brilliant III Ultra-Fast SYBR® Green QPCR Master Mix (Agilent) and the following primer pairs: *HNRNPL_NMD*, FW 5'-GGTCGCAGTGTATGTTTGATG-3' and RW 5'-GGCGTTTGTTGGGGTTGCT-3'; TRA2B_NMD, FW 5'-TGGAATCAGAAAGCACTACGC-3' and RW 5'-GAATCTTCCTTGGAGCGAGA-3'; *HNRNPL_PROT*, FW 5'-CAATCTCAGTGGACAAGGTG-3' and RW 5'-CTCCATATTCTGCGGGGTGA-3'; and *TRA2B_PROT*, FW 5'-GAGGTTGGCAGCTTCGATT-3' and RW 5'-AAGCAGAACGGGATTCCC-3'. Expression levels were normalized to the average level of *β-actin* (*ACTB*) as internal control FW 5'-ACGGCTCCGGCATGTGCAAG-3' and RW TGACGATGCCGTGCTCGATG.

**References**

[1] Grohmann K, Schuelke M, Diers A, Hoffmann K, Lucke B, Adams C et al (2001) Mutations in the gene encoding immunoglobulin mu-binding protein 2 cause spinal muscular atrophy with respiratory distress type 1. Nat Genet 29:75-77.

[2] Maury Y, Côme J, Piskorowski RA, Salah-Mohellibi N et al (2015) Combinatorial analysis of developmental cues efficiently converts human pluripotent stem cells into multiple neuronal subtypes. Nat Biotechnol 33(1):89-96.

[3] Nizzardo M, Simone C, Rizzo F, Salani S, Dametti S, Rinchetti P et al (2015) Gene therapy rescues disease phenotype in a spinal muscular atrophy with respiratory distress type 1 (SMARD1) mouse model. Sci Adv 1(2):e1500078.

[4] Linde L, Boelz S, Neu-Yilik G, Kulozik AE, Kerem B (2007) The efficiency of nonsense-mediated mRNA decay is an inherent character and varies among different cells. Eur J Hum Genet 15(11):1156-62.